

Article

Insights in the Rhodium-Catalyzed Tandem Isomerization-Hydroformylation of 10-Undecenitrile: Evidence for a Fast Isomerization Regime

Lucas Le Goanvic ¹, Jean-Luc Couturier ², Jean-Luc Dubois ³ and Jean-François Carpentier ^{1,*} 

¹ Organometallics, Materials and Catalysis, UMR 6226 Institut des Sciences Chimiques de Rennes, CNRS-University of Rennes 1, F-35042 Rennes, France; lucas.legoanvic@gmail.com or lucas.le-goanvic@univ-rennes1.fr

² Arkema France, CRRA, BP 63, Rue Henri Moissan, F-69493 Pierre Bénite, France; jean-luc.couturier@arkema.com

³ Arkema France, 420 Rue d'Estienne d'Orves, F-92705 Colombes, France; jean-luc.dubois@arkema.com

* Correspondence: jean-francois.carpentier@univ-rennes1.fr or jcarpent@univ-rennes1.fr; Tel.: +33-223-233-748

Received: 20 March 2018; Accepted: 2 April 2018; Published: 5 April 2018



Abstract: The tandem isomerization-hydroformylation of 10-undecenitrile (**1**) into the corresponding linear aldehyde (**2**) with a Rh-biphephos system was studied and the formation of internal olefin isomers (**1-int-x**) was monitored over time. The existence of an “isomerization phenomenon” was evidenced, where fast isomerization of **1** into up to 70% of **1-int-x** followed by fast back-isomerization of **1-int-x** into **1** and, in turn, into **2** occurs. This fast dynamic isomerization regime is favored at high syngas pressure (40 bar) and low biphephos-to-Rh ratio (5–10), and it is best observed at relatively high catalyst loadings ($[1]_0/[Rh] \leq 3000$). The latter regime is indeed evanescent, and gives place to a second stage in which isomerization of internal olefins (and eventual conversion into **2**) proceeds much more slowly. The results are tentatively rationalized by the formation of an unstable species that promotes dynamic isomerization and which slowly vanishes or collapses into a Rh-biphephos species which is the one responsible for hydroformylation.

Keywords: tandem reaction; hydroformylation; isomerization; rhodium; biphephos; undecenitrile

1. Introduction

The increasing complexity of olefin substrates used in hydroformylation has introduced new challenges over the last decades. In particular, the production of linear (terminal) aldehydes from long-chain (“fatty”) olefins raises the issue of internal alkenes that may be present in initial feedstocks or that almost always form during the hydroformylation process [1]. Hence, to reach high selectivities and conversions toward the desired linear aldehyde, a tandem process is required, in which dynamic isomerization and (essentially) irreversible hydroformylation reactions must be effectively coupled [2,3]. This approach proved in several instances to be a synthetically quite effective strategy, through tuning of the catalyst system and optimizing the reaction conditions [4–17]. However, the fundamentals of this process such as detailed speciation of organic products over time, kinetics, were rarely investigated [11].

Our own work in that field is focused on the tandem isomerization-hydroformylation of 10-undecenitrile (**1**), a bio-sourced unsaturated fatty nitrile that can be used as an entry toward valuable polymers. In fact, the linear aldehyde product (**2**) obtained can be readily converted to prepare the monomer for polyamide-12. For this purpose, the amount of byproducts, i.e., branched aldehydes (**3**) (under regular conditions, i.e., when the reaction temperature was not forced, only aldehydes resulting from the terminal olefin (**1**) were observed; branched aldehydes in deeper (≤ 8 -

positions, resulting from the hydroformylation of internal olefins (**1-int-x**), were observed only at $T > 140\text{ }^{\circ}\text{C}$; see [18,19]), internal alkenes (**1-int-x**) and hydrogenated products (**4**), must be minimized (Figure 1). The challenge to optimize the reaction regioselectivity (defined as the linear-to-branched aldehyde ratio, l/b ; (**2**)/(**3**)) and chemoselectivity (defined as hydroformylation vs. all other processes; %HF) is high as, in this case, the starting material contains already ca. 5–7% of internal alkenes (essentially 9-undecenitrile), inherent to its production mode [20].

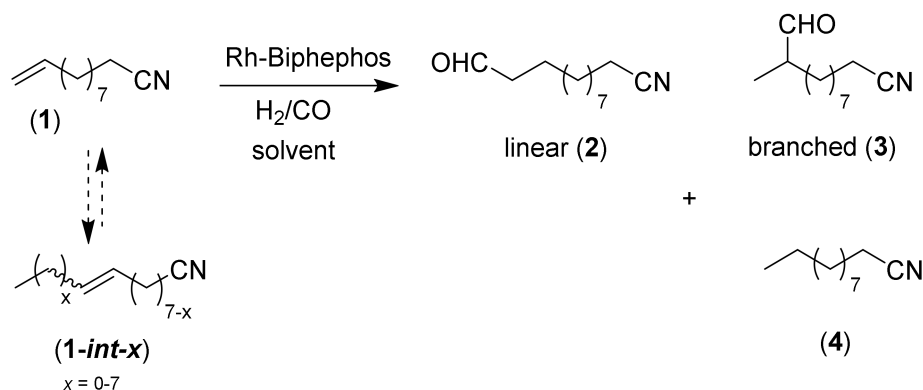


Figure 1. Illustration of the main products obtained from the Rh-catalyzed hydroformylation of 10-undecenitrile (**1**).

In our previous works, excellent regioselectivity with l/b values up to 99:1 could be obtained using combinations of the ubiquitous biphephos ligand with rhodium [18], iridium [21] or ruthenium [19] precursors. This was achieved under optimized conditions, quite similar for all three systems, typically $[\mathbf{1}]_0 = 1.0\text{ M}$, $[\mathbf{1}]_0/[\text{Rh or Ir}] = 20,000$, $[\text{biphephos}]/[\text{M}] = 20$, 20 bar CO/H₂ (1:1), $T = 120\text{ }^{\circ}\text{C}$. If the productivity and regioselectivity values stand among the best for hydroformylation of this kind of long chain olefins, the chemoselectivity (77% for the Rh-biphephos) remains, however, lower. In particular, large amounts of internal olefins (**1-int-x**; typically 20–25%) are still present in final mixtures. As anticipated, it proved possible to decrease the amounts of internal alkenes with the Rh-biphephos system by increasing sequentially the reaction temperature; hence, the yield of aldehydes raised up to 84% (with a constant high regioselectivity) but major amounts of hydrogenated product **4** (12%) were formed concomitantly [18]. Thus, developing a strategy for the consumption of internal alkenes is an important, general objective for tandem isomerization–hydroformylation processes.

In this work, a kinetic monitoring of the competitive reactions taking place during the tandem isomerization-hydroformylation of 10-undecenitrile was systematically undertaken. Interestingly, under specific conditions, a fast isomerization regime was evidenced in the early stages of the process. Detailed studies conducted around this observation are presented below.

2. Results and Discussion

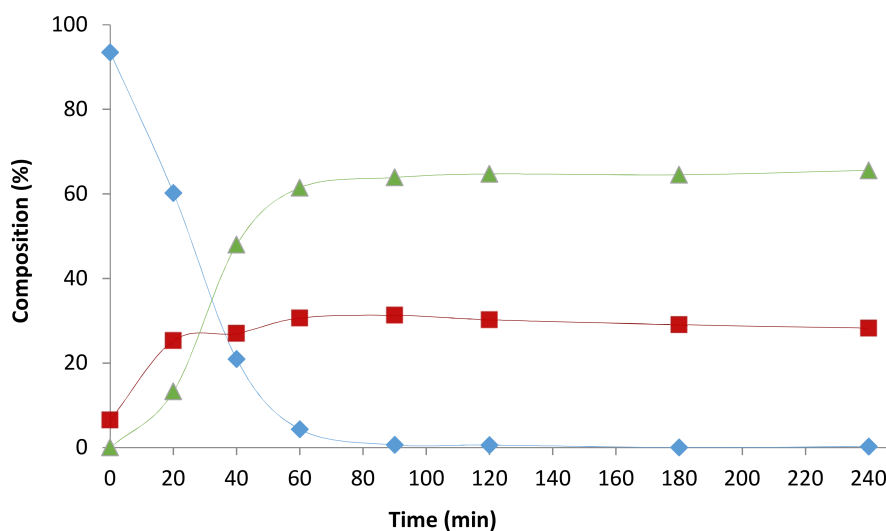
2.1. Preliminary Notes

In order to observe roughly similar overall reaction rates when the $[\mathbf{1}]_0/[\text{Rh}]$ ratio was modified from the regular value of 20,000 (referred to as “standard conditions”) to higher catalyst loadings (referred to as “isomerizing conditions”), the catalyst and substrate concentrations were adjusted so that the same product $[\mathbf{1}]_0 \times [\text{Rh}]$ ($5 \times 10^{-5}\text{ M}^2$) is achieved (this was made assuming a pseudo-first order for the substrate and the catalyst and an overall reaction rate expressed as $r = k_{\text{app}}' \times [\mathbf{1}]^1 \times [\text{Rh}]^1$). Other parameters (temperature, pressure, $[\text{biphephos}]/[\text{Rh}]$, etc.) were not modified in a first instance. As reproducibility was important to probe, the composition profiles presented in the section below are typically superposition of data collected from at least three different experiments run under the same conditions. To measure the importance of hydroformylation vs. isomerization,

initial turnover frequencies of each process were determined: $\text{TOF}_{\text{iso}}^0$ for isomerization (apparent formation of **1-int-x**) and TOF_{HF}^0 for hydroformylation (formation of **2 + 3**). Note that these values were determined at the maximum slope ($\text{TOF}_{\text{iso}}^0 = \frac{\%(\mathbf{1-int-x})_{\text{formed}} \times \frac{[\mathbf{1}]}{[\text{Rh}]}}{t(h)}$; $\text{TOF}_{\text{HF}}^0 = \frac{\%(2+3) \times \frac{[\mathbf{1}]}{[\text{Rh}]}}{t(h)}$); hence, as the two values were not necessarily measured at the same time (the maximum slope can occur after different time), the sum of $\text{TOF}_{\text{iso}}^0 + \text{TOF}_{\text{HF}}^0$ can be higher than the overall TOF (determined from the conversion of **1** at its maximal slope). Note also that TOF_{iso} is a minimal apparent value, since interconversion of internal olefins $\mathbf{1-int-x} \rightleftharpoons \mathbf{1-int-x'}$ is not observed by ^1H NMR spectroscopy.

2.2. Influence of the $[\mathbf{1}]_0/[\text{Rh}]$ Ratio

The change in the catalyst loading and reactant concentrations induced an unexpected change in the composition profile. Under “standard conditions” ($[\mathbf{1}]_0/[\text{Rh}] = 20,000$; $[\mathbf{1}]_0 = 1.0$ M), isomerization proceeded apparently more slowly and in parallel to hydroformylation ($\text{TOF}_{\text{HF}}^0 > \text{TOF}_{\text{iso}}^0$, see Figure 2). On the contrary, under “isomerizing conditions” (at $[\mathbf{1}]_0/[\text{Rh}] = 3000$; $[\mathbf{1}]_0 = 0.4$ M for instance), the isomerization process was clearly more pronounced in the first stages of the reaction ($\text{TOF}_{\text{HF}}^0 = 2585 \text{ h}^{-1} < \text{TOF}_{\text{iso}}^0 = 4656 \text{ h}^{-1}$; see Figure 2) and a significant amount of internal isomers **1-int-x** built up in the reaction mixture, e.g., up to 41% after ca. 20 min. In the latter case, when the terminal olefin (**1**) was exhausted, a fast decrease of the internal olefins concentration previously produced was noted, while concomitantly aldehydes continued to form. Hence, most importantly, this additional amount of aldehydes formed came (at least in a significant part) from internal isomers that were back-isomerized into **1**, which was then in turn rapidly and irreversibly transformed into **2** (along with a minor amount of **3**). The high *l/b* ratio (99.2:0.8) is an evidence of this process. This regime of fast decrease in internal isomers lasts for ca. 20–60 min and then returns progressively to the “standard” regime of slow internal olefins conversion (and slow production of **2**), as that observed at $[\mathbf{1}]_0/[\text{Rh}] = 20,000$. Figure 2 below illustrates the difference in composition profiles under the different conditions (for the sake of clarity, the amount of hydrogenated product **4** over time was removed as it was similar in both conditions (a smooth and regular increase to reach ca. 5% in final mixture)).



(a)

Figure 2. Cont.

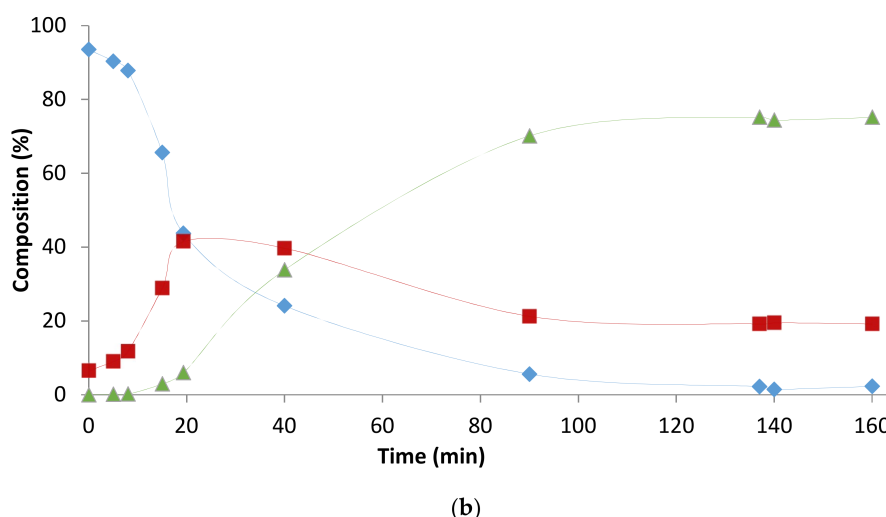


Figure 2. Differences in composition profile as a function of time between the Rh-biphephos system in toluene: (a) at $[1]_0/[Rh] = 20,000$; (b) at $[1]_0/[Rh] = 3000$; (♦ 1, ■ 1-int-x, ▲ 2 + 3).

Figure 3 shows the extent of the “isomerization peak” as a function of the $[1]_0/[Rh]$ ratio (20,000; 7000; 3000; 1000; 333), always keeping the same $[1]_0 \times [Rh]$ product ($[1]_0 \times [Rh] = 5.10^{-5} \text{ M}^2$). For all $[1]_0/[Rh]$ ratios ≤ 7000 , the same observation was made and the lower the $[1]_0/[Rh]$ ratio, the more important the phenomenon. An experiment was conducted, at $[1]_0/[Rh] = 20,000$ and $[1]_0 = 0.4 \text{ M}$, but no isomerization was observed. This demonstrates the essential impact of the ratio $[1]_0/[Rh]$ on the possibility to observe such isomerization phenomenon. When this phenomenon was observed, the $\text{TOF}_{\text{iso}}^0/\text{TOF}_{\text{HF}}^0$ ratio was generally found higher than ca. 1.8 (see Table 1). The extent of isomerization can also be evaluated by the amount of the internal isomers present in the reaction mixture after ca. 20 min, i.e., at the “isomerization peak”. Hence, the maximal amount of 1-int-x rose in between 38% and 66%. The final chemoselectivities for aldehydes (ca. 80%) and internal isomers (ca. 20%) were, respectively, slightly improved and decreased, when compared to those observed under “standard conditions”. Thus, the lower the $[1]_0/[Rh]$ ratio, the higher the chemoselectivity (%HF).

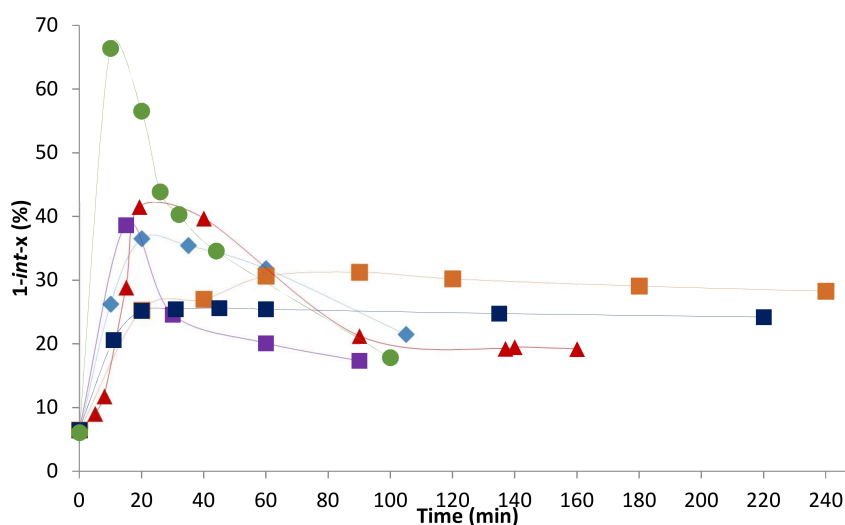


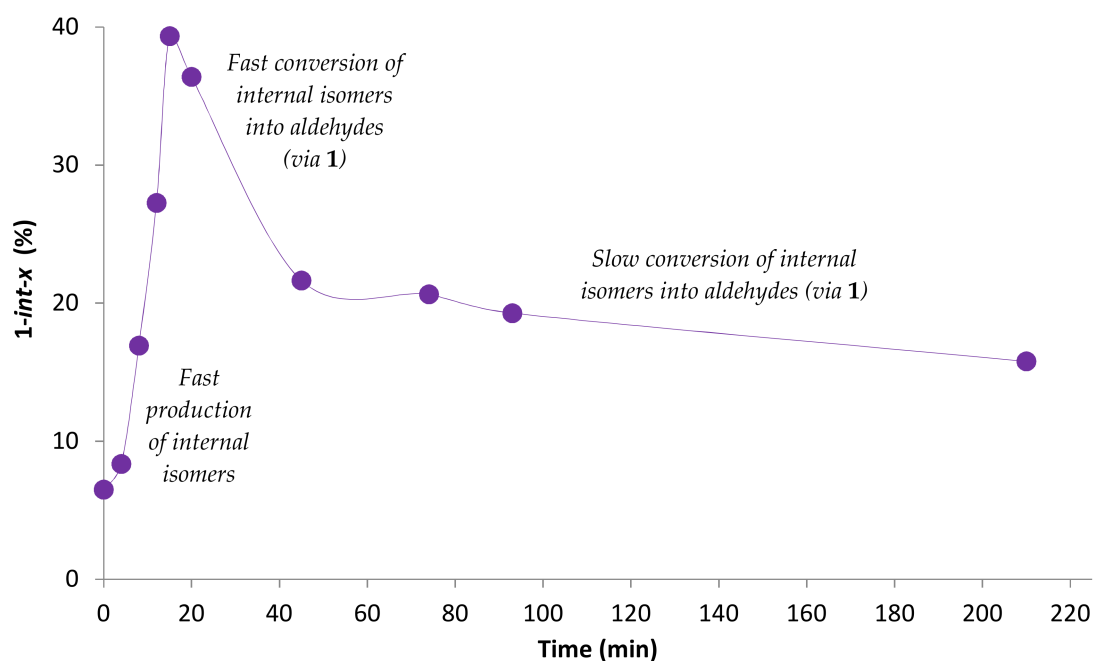
Figure 3. Influence of the $[1]_0/[Rh]$ ratio on the amount of internal isomers (1-int-x) as a function of time in tandem isomerization-hydroformylation of 10-undecenitrile (■ $[1]_0/[Rh] = 20,000$ (1.0 M), ■ $[1]_0/[Rh] = 20,000$ (0.4 M), ♦ $[1]_0/[Rh] = 7000$, ▲ $[1]_0/[Rh] = 3000$, ■ $[1]_0/[Rh] = 1000$, ● $[1]_0/[Rh] = 333$).

Table 1. Influence of the $[1]_0/[Rh]$ ratio on tandem isomerization-hydroformylation of 10-undecenitrile ¹.

Entry	$[1]_0/[Rh]$	$[1]_0$	Time	1	1-int-x	[2] + [3]	[2]/[3]	4	Conv. 1	HF	TOF	TOF ^{iso}	TOF ^{HF}
	Ratio	[mol·L ⁻¹]	[h]	[%] ²	[%] ²	[%] ²	(l/b) ³	[%] ²	[%] ⁴	[%] ⁵	[h ⁻¹] ⁶	[h ⁻¹] ⁷	[h ⁻¹] ⁷
entry 1	20,000	1.00	1.5	1	25	68	99.0:1.0	6	99	74	28,250	7900	17,050
entry 2	7000	0.59	1.75	9	21	66	99.2:0.8	3	90	79	10,100	8500	1600
entry 3	3000	0.40	2.33	2	19	75	99.2:0.8	4	99	82	7850	4650	2600
entry 4	1000	0.23	1.5	0	17	76	99.1:0.9	7	100	81	3450	1300	1750
entry 5	335	0.12	1.67	0	18	78	99.1:0.9	4	100	84	1800	1200	450
entry 6	20,000	0.40	3.67	2	24	69	99.1:0.9	5	98	76	20,100	8650	15,500

¹ Reaction conditions unless otherwise stated: $[1]_0/[1-int-x]_0 = 93.5:6.5$, $[biphephos]_0/[Rh] = 20$, $T = 120$ °C, $P = 20$ bar CO/H_2 (1:1). ² Distribution (mol%) of remaining **1**, internal alkenes **1-int-x** (residual or formed during the reaction), aldehydes **2** and **3**, and hydrogenation product **4**, as determined by NMR analyses. ³ Regioselectivity as determined by the linear-to-branched aldehyde ratio. ⁴ Conversion of **1**. ⁵ Chemoselectivity as determined by the percentage of hydroformylation among all other competitive processes. ⁶ TOF determined from the conversion of **1** at its maximal slope. ⁷ TOF of each process determined from the formation of the corresponding product at the maximal slope.

Overall, two main kinetic regimes can be defined regarding the amount of internal alkenes (see Figure 4): (i) a first stage (typically before ca. 45 min) with rapid isomerization of the unsaturated carbon chain in both directions and (ii) a second stage (typically after ca. 45 min) where the consumption of internal isomers proceeds much more slowly. The first stage can be in turn decomposed in two periods: a fast building up of internal isomers (before ca. 20 min) followed by a fast consumption of these isomers (between ca. 20 and 45 min) that occurs when the terminal isomer (**1**) is exhausted. This last regime is remarkable as it evidences the existence of a relatively short time period during which fast reversible isomerization of internal olefins (along with hydroformylation) is very effective. To our knowledge, evidence for this fast regime is a unique example to date in tandem isomerization-hydroformylation of long chain internal olefins into linear aldehydes (with a high regioselectivity: $l/b \approx 99.0:1.0$ constant throughout the reaction process).

**Figure 4.** Schematic representation of the “isomerization phenomenon”.

Since the central objective of tandem isomerization-catalytic processes is to convert all internal alkenes into the final products, this observation is of paramount importance: indeed, the capacity to maintain the fast internal isomers consumption regime until quantitative conversion would be a most promising achievement. The observation of two different regimes during the course of the

reaction may account for the existence of (at least) two different catalytic species: we hypothesize that, in addition to the regular hydroformylation catalyst (likely a single one, as evidenced by the constant l/b ratio throughout the reaction), a catalytic species that strongly promotes isomerization could be efficiently operating in the first stages of the reaction (*vide infra*).

In order to gain a better understanding of this “isomerization phenomenon”, further experiments were conducted by modifying the operational parameters. In light of the above results, all subsequent reactions were performed at $[1]_0/[Rh] = 3000$ and $[1]_0 = 0.4$ M.

2.3. Solvent Effects

When acetonitrile and 1,4-dioxane were used as solvents in place of toluene, the isomerization peak was still observed. For the sake of clarity, only the amount of internal isomers over time is plotted in each solvent in Figure 5 (see Table 2 and the Appendix A for the complete compositions profiles). The phenomenon appears even sharper with these solvents, as the consumption of internal isomers is considerably fastened as compared to toluene (the fast consumption period last only ca. 10 min compared to 70 min) and the maximal amount of **1-int-x** in these solvents was above 50%. The TOFs of each catalytic process that illustrate this trend are reported in Table 2. This apparent solvent effect may in fact arise from different hydroformylation rates, thus affecting the equilibrium $\mathbf{1-int-x} \rightleftharpoons \mathbf{1} \rightarrow \mathbf{2}$.

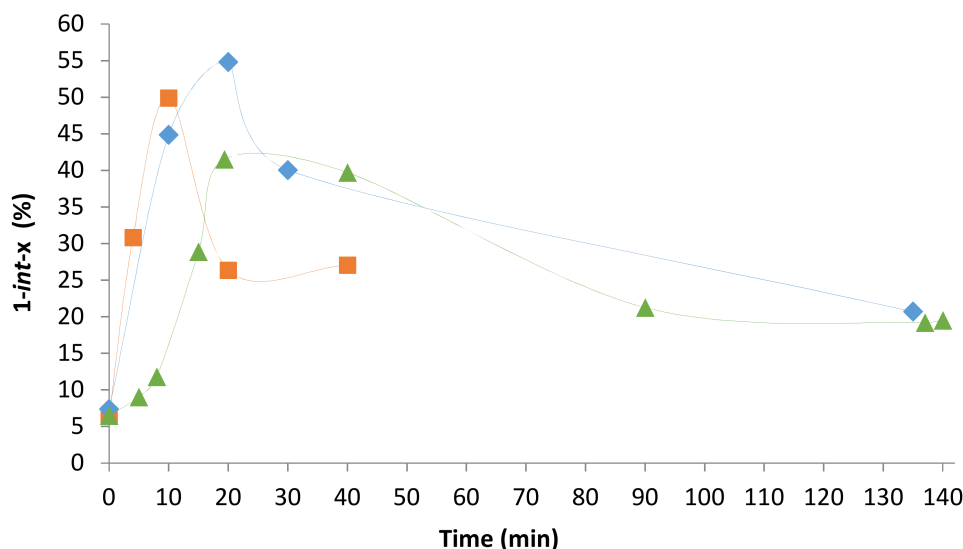


Figure 5. Influence of the solvent on the amount of internal isomers (**1-int-x**) as a function of time in tandem isomerization-hydroformylation of 10-undecenitrile at $[1]_0/[Rh] = 3000$ (◆ 1,4-dioxane, ■ acetonitrile, ▲ toluene).

Table 2. Influence of the solvent on tandem isomerization-hydroformylation of 10-undecenitrile at $[1]_0/[Rh] = 3000$ ¹.

Entry	Solvent	Time [h]	1	1-int-x	2 + 3	$[2]/[3]$ (l/b) ³	4	Conv. 1	HF	TOF	TOF _{iso} ⁰	TOF _{HF} ⁰
			[%] ²	[%] ²	[%] ²		[%] ²	[%] ⁴	[%] ⁵	[h ⁻¹] ⁶	[h ⁻¹] ⁷	[h ⁻¹] ⁷
entry 7	toluene	2.33	2	19	75	99.2:0.8	4	99	82	7850	4650	2600
entry 8	MeCN	0.67	1	27	68	99.4:0.6	4	99	74	17,800	10,950	7450
entry 9	1,4-dioxane	2.25	1	21	74	99.2:0.8	5	99	81	6650	6750	2150

¹ Reaction conditions unless otherwise stated: $[1]_0/[1-int-x]_0 = 93.5:6.5$, $[1]_0 = 0.4$ M at $[1]_0/[Rh] = 3000$, [biphospho]/[Rh] = 20, T = 120 °C, P = 20 bar CO/H₂ (1:1). ² Distribution (mol%) of remaining **1**, internal alkenes **1-int-x** (residual or formed during the reaction), aldehydes **2** and **3**, and hydrogenation product **4**, as determined by NMR analyses. ³ Regioselectivity as determined by the linear-to-branched aldehyde ratio. ⁴ Conversion of **1**. ⁵ Chemoselectivity as determined by the percentage of hydroformylation among all other competitive processes. ⁶ TOF determined from the conversion of **1** at its maximal slope. ⁷ TOF of each process determined from the formation of the corresponding product at the maximal slope.

2.4. Pressure Variation

Syngas pressure is of major importance in hydroformylation, in particular on the presence or life-time of catalytic species [2,22]. The latter parameter was varied from 4 to 40 bar, keeping the CO/H₂ feed ratio at 1:1. Monitoring of the reactions over time still evidenced the “isomerization phenomenon”; however, the profiles were clearly pressure-dependent, as presented in Figure 6 (for the sake of clarity, only the amount of internal isomers over time is plotted at each pressure).

At relatively high pressure (20 and 40 bar), large amounts of **1-int-x** were formed (up to 42% and 39%, respectively), and a fast decrease followed by a slower consumption of these internal isomers was then noticed. The final amounts reached after 2–3 h of reaction were in the same range (19% and 16%, respectively). On the other hand, at lower pressure (4 and 8 bar), the amounts of **1-int-x** formed were also high (up to 42% and 51%, respectively), but their concentration decreased more slowly and the final amounts reached after 2 h reaction remained important (42% and 35%, respectively). Hence, the higher the syngas pressure, the more apparent the “isomerization phenomenon”. One can hypothesize that this pressure effect could just result from different hydroformylation rates; in other words, the overall pressure does not affect the isomerization rate (as evidenced by the similar initial slopes; see Figure 6), but does for the hydroformylation rate: the higher the pressure, the faster the hydroformylation and, hence, the capacity to drive the equilibrium $\mathbf{1-int-x} \rightleftharpoons \mathbf{1} \rightarrow \mathbf{2}$.

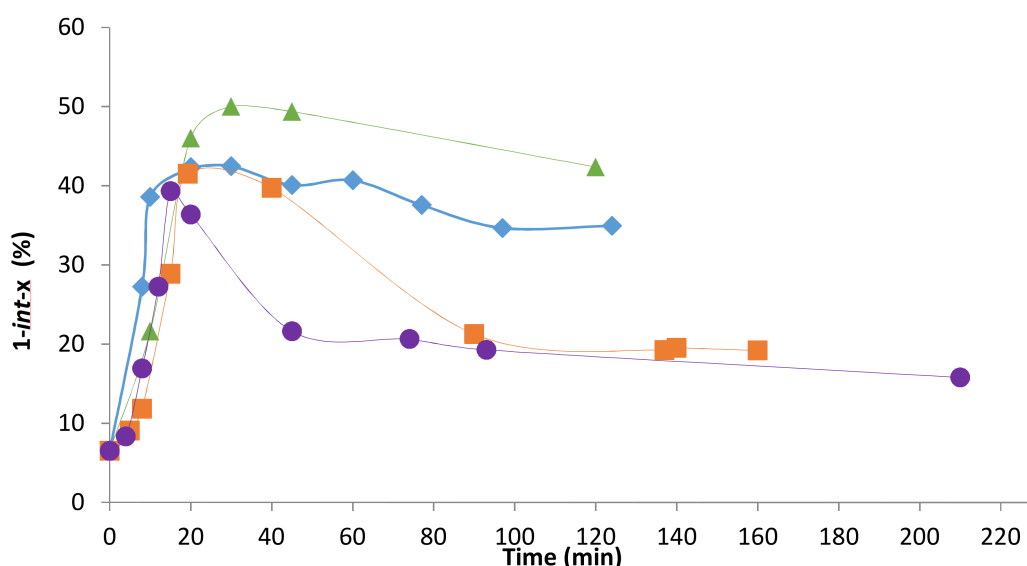


Figure 6. Influence of syngas pressure (CO/H₂ = 1:1) on the amount of internal isomers (**1-int-x**) as a function of time in tandem isomerization-hydroformylation of 10-undecenitrile at [1]₀/[Rh] = 3000 (▲ 4 bar, ◆ 8 bar, ■ 20 bar, ● 40 bar).

Additional experiments performed at different CO/H₂ ratios (3:1 and 1:3), maintaining an overall pressure of 40 bar, returned composition profiles similar to those of experiments conducted at 1:1 ratio (see the Appendix A). Thus, no major influence of carbon monoxide and/or hydrogen could be established. On the other hand, as expected, an important amount of hydrogenated product **4** (9%) at CO/H₂ = 1:3 was noticed; on the contrary, this amount was low (2%) at CO/H₂ = 3:1.

The TOF⁰s of each catalytic process, as well as the composition of final mixtures and final chemoselectivity (%HF) and regioselectivity (*l/b* ratio), are reported in Table 3. In all cases, isomerization proceeded faster than hydroformylation. If the final regioselectivity values were very similar at any pressure, at low pressure internal alkenes were not consumed fast, resulting in poor chemoselectivity (63% and 54% at 8 and 4 bar, respectively). Above 20 bar, final selectivities were in the same range.

Table 3. Influence of syngas pressure on tandem isomerization-hydroformylation of 10-undecenitrile at $[1]_0/[Rh] = 3000$ ¹.

Entry	P	CO/H ₂	Time	1	1-int-x	2 + 3	[2]/[3] (l/b) ³	4	Conv. 1	HF	TOF	TOF ⁰ _{iso}	TOF ⁰ _{HF}
	[bar]	Ratio	[h]	[%] ²	[%] ²	[%] ²		[%] ²	[%] ⁴	[%] ⁵	[h ⁻¹] ⁶	[h ⁻¹] ⁷	[h ⁻¹] ⁷
entry 10	4	1:1	2	2	42	50	99.1:0.9	6	99	54	6650	3550	2450
entry 11	8	1:1	2	1	35	58	99.0:1.0	6	99	63	1140	5800	4300
entry 12	20	1:1	2.67	2	19	75	99.2:0.8	3	98	82	7850	4650	2600
entry 13	40	1:1	3.5	0	16	79	98.6:1.4	5	100	85	6750	3950	2950
entry 14	40	3:1	3.67	1	18	78	98.8:1.2	2	98	85	3000	2300	1400
entry 15	40	1:3	2.5	2	18	71	99.1:0.9	9	97	75	6000	4500	1700

¹ Reaction conditions unless otherwise stated: $[1]_0/[1-int-x]_0 = 93.5:6.5$; $[1]_0 = 0.4$ M, $[1]_0/[Rh] = 3000$, $[biphephos]_0/[Rh] = 20$, toluene (8 mL), T = 120 °C. ² Distribution (mol%) of remaining **1**, internal alkenes **1-int-x** (residual or formed during the reaction), aldehydes **2** and **3**, and hydrogenation product **4** as determined by NMR analyses. ³ Regioselectivity as determined by the linear-to-branched aldehyde ratio. ⁴ Conversion of **1**. ⁵ Chemoselectivity as determined by the percentage of hydroformylation among all other competitive processes. ⁶ TOF determined from the conversion of **1** at its maximal slope. ⁷ TOF of each process determined from the formation of the corresponding product at the maximal slope.

2.5. [Biphephos]/[Rh] Variation

Monitoring of reactions performed with $[biphephos]/[Rh]$ ratios in the range 5 to 50 showed that the “isomerization phenomenon” is highly dependent on this parameter. This is illustrated in Figure 7; here again, for the sake of clarity, only the amount of internal isomers over time is plotted at each ratio. The lower the $[L]/[Rh]$ ratio, the higher and the sharper the formation of internal isomers is. With 5 equiv. of biphephos vs. rhodium, the amount of **1-int-x** reached 64% after 20 min, immediately followed by a fast decay of such species. On the contrary, at $[L]/[Rh] = 50$, almost no isomerization peak was observed (maximal amount of **1-int-x** = 22%) and the composition profile was very similar to that observed at $[1]_0/[Rh] = 20,000$.

The TOFs of the catalytic process that illustrate this trend are reported in Table 4. Importantly, at low $[biphephos]/[Rh]$ ratio, the isomerization rate was much more important than the hydroformylation rate; this is not any longer the case at higher $[biphephos]/[Rh]$ ratio (entry 19). On the other hand, the final amount of internal alkenes was very similar regardless the $[biphephos]/[Rh]$ ratio (18–20% for all experiments). The final chemoselectivity and regioselectivity values were also very similar for all these experiments.

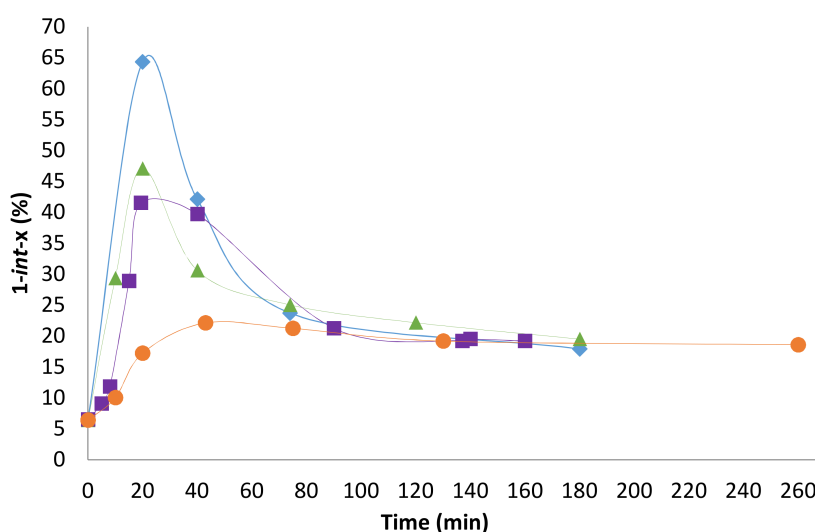


Figure 7. Influence of the $[biphephos]/[Rh]$ ratio ($[L]/[M]$) on internal isomers (**1-int-x**) as a function of time in tandem isomerization-hydroformylation of 10-undecenitrile at $[1]_0/[Rh] = 3000$ (♦ $[L]/[M] = 5$, ▲ $[L]/[M] = 10$, ■ $[L]/[M] = 20$, ● $[L]/[M] = 50$).

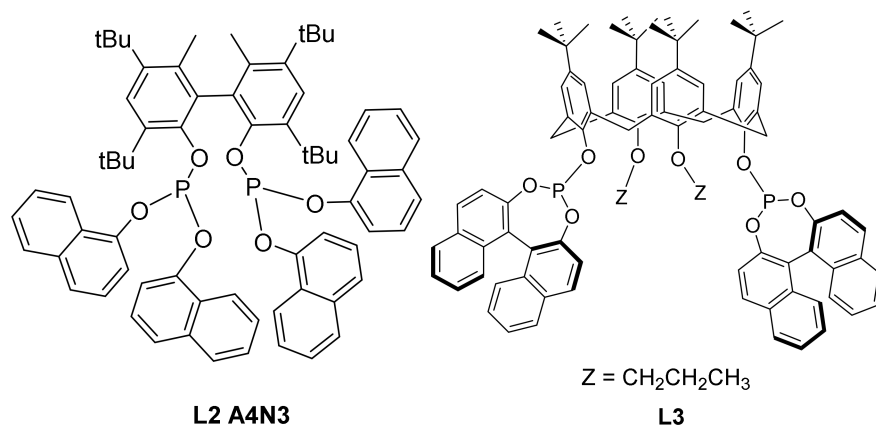
Table 4. Influence of the [biphephos]/[Rh] ratio on tandem isomerization-hydroformylation of 10-undecenitrile at $[1]_0/[Rh] = 3000$ ¹.

Entry	[L]/[M]	Time	1	1-int-x	2 + 3	[2]/[3]	4	Conv. 1	HF	TOF	TOF ^{iso}	TOF ^{HF}
	Ratio	[h]	[%] ²	[%] ²	[%] ²	(<i>l/b</i>) ³	[%] ²	[%] ⁴	[%] ⁵	[h ⁻¹] ⁶	[h ⁻¹] ⁶	[h ⁻¹] ⁷
entry 16	5	3	1	18	77	99.3:0.7	4	99	84	7850	5200	2300
entry 17	10	3	1	20	76	99.2:0.8	5	99	82	5050	4150	1650
entry 18	20	2.7	2	19	75	99.2:0.8	3	98	82	7850	4650	2600
entry 19	50	4.3	3	19	75	99.1:0.9	3	97	83	2350	1000	1450

¹ Reaction conditions unless otherwise stated: $[1]_0/[1-int-x]_0 = 93.5:6.5$, $[1]_0 = 0.4$ M $[1]_0/[Rh] = 3000$, P = 20 bar (CO/H₂ = 1:1), toluene (8 mL), T = 120 °C. ² Distribution (mol%) of remaining **1**, internal alkenes **1-int-x** (residual or formed during the reaction), aldehydes **2** and **3**, and hydrogenation product **4**, as determined by NMR analyses. ³ Regioselectivity as determined by the linear-to-branched aldehyde ratio. ⁴ Conversion of **1**. ⁵ Chemoselectivity as determined by the percentage of hydroformylation among all other competitive processes. ⁶ TOF determined from the conversion of **1** at its maximal slope. ⁷ TOF of each process determined from the formation of the corresponding product at the maximal slope.

2.6. Other Effects: Ligands, Substrates

In addition to the abovementioned effects on the isomerization phenomenon, the influence of other parameters was explored. The fast dynamic isomerization regime was observed also with other bulky biphosphite ligands (Figure 8). A calixarene-type ligand (**L2**) developed by Sémeril and Matt [9,23] returned a behavior quite similar to that of biphephos (for reactions performed in toluene or acetonitrile); a somewhat less pronounced, yet clearly visible, effect was observed using the **A4N3** ligand, another efficient biphosphite ligand used in tandem isomerization-hydroformylation reactions [17] (see the Appendix A).

**Figure 8.** Other biphosphite ligands investigated in the tandem isomerization-hydroformylation of 10-undecenitrile.

On the contrary, the isomerization phenomenon proved to be strictly substrate-dependent. Indeed, nothing comparable was observed using methyl 10-undecenoate or 5-hexenenitrile (Figure 9), two substrates closely related to 10-undecenitrile; in those cases, the hydroformylation rate was higher than the apparent isomerization rate, and there was no building up of internal olefins, at least under the reaction conditions investigated (see the Appendix A). Since the only difference between 10-undecenitrile and methyl 10-undecenoate is the terminal function, the tandem isomerization-hydroformylation of methyl 10-undecenoate was also investigated in acetonitrile as solvent, to investigate a possible role of the nitrile function. However, here again, no “isomerization peak” was observed (see the Appendix A) (the absence of isomerization phenomenon with substrates other than 10-undecenitrile may raise questions about the possible presence of impurities and their possible role in the observed phenomenon. It is important to note that the studies here reported were performed with different batches of 10-undecenitrile, which all returned HF reproducible and consistent

results. To remove any doubt, different purification protocols of the starting material were performed prior to use in catalysis; in particular, 10-undecenitrile was systematically eluted through a short pad of activated neutral alumina (to remove peroxides) and vacuum distilled (Kügelrohr; 125 °C, 0.03 mmHg). Additional elimination of peroxides was performed by heating the distilled substrate at 150 °C under argon overnight. All differently-purified batches of 10-undecenitrile returned reproducible and consistent results.).

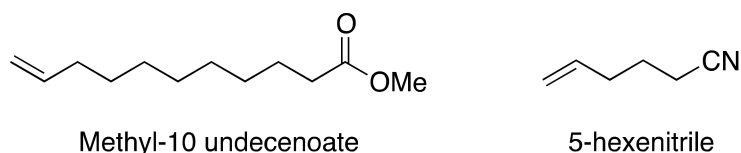


Figure 9. Methyl 10-undecenoate and 5-hexenenitrile; other substrates investigated in this study.

2.7. Investigations on the Catalytic Species

In the vast majority of cases reported in the literature, hydroformylation catalysts are generated *in situ* by exposition of combinations of the metal precursor and ligand to a syngas pressure [2,3]. In our procedure, a precatalyst species is formed before introduction of reactants by mixing 20 equiv. of biphosphos with $\text{Rh}(\text{acac})(\text{CO})_2$ [18]. In addition to this regular procedure, the reaction was also investigated with $\text{RhH}(\text{biphosphos})(\text{CO})_2$, the “resting state” species which was previously prepared by treating $\text{Rh}(\text{acac})(\text{CO})_2$ with 1.5 equiv. of biphosphos under syngas pressure (20 bar, 120 °C, toluene [18]). This isolated species was used in isomerizing studies alone or with addition of extra biphosphos (20 equiv.). In both cases, the isomerization phenomenon was observed, although the isomerization peak was clearly less pronounced than with *in situ* generated catalyst systems (see the Appendix A).

Monitoring of the reaction by ^{31}P NMR at high pressure was also attempted (thanks to the group of Pr. Carmen Claver and Dr. Cyril Godard from the University of Tarragona) in order to confirm or infirm the hypothesis of different catalytic species: one responsible for fast dynamic isomerization and another one essentially active in hydroformylation. Unfortunately, it did not allow us to identify unambiguously any of such species, despite experiments carried out under different conditions (see the Appendix A).

3. Materials and Methods

3.1. General Considerations

Toluene was purified over alumina columns using an MBraun system (M. Braun Inertgas-Systeme GmbH, Garching, Germany). Acetonitrile and 1,4-dioxane were dried over CaH_2 , distilled, and stored in a Schlenk flask under an inert atmosphere and over molecular sieves. All reactions involving Rh catalysts were performed under an inert atmosphere (argon) using standard Schlenk techniques. $\text{Rh}(\text{acac})(\text{CO})_2$ was generously provided by Umicore (Hanau-Wolfgang, Germany) or purchased from Strem Chemicals (Newburyport, MA, USA) and stored under air. Biphosphos was purchased from Aldrich Chemicals (St. Louis, MO, USA) and Strem Chemicals (Newburyport, MA, USA) and stored in a glove box. The A4N3 ligand was purchased from MCAT GmbH (Donaueschingen, Germany) and used as received. The calixarene-type bisphosphite ligand L2 was provided by Dr David Sémeril and Dr Dominique Matt from the University of Strasbourg (*Laboratoire de Chimie Inorganique Moléculaire et Catalyse*, UMR 7177) and used as received. 10-Undecenitrile (typically 93.5% pure, contains 6.5% of 9-undecenitrile, as determined by NMR) and methyl 10-undecenoate (>99% of terminal alkene as determined by NMR) were supplied by Arkema Co. (Colombes, France); they were first eluted through a short alumina column and vacuum-distilled (Kügelrohr distillation under 0.03 mm Hg at 125 °C) prior to use. 5-Hexenenitrile was purchased from Aldrich Chemicals (St. Louis, MO, USA) and elution through a short neutral alumina column before use. ^1H , ^{13}C NMR and ^{31}P NMR spectra were

recorded on Bruker AC-300 and AM-400 spectrometers (Bruker, Wissembourg, France). ^1H and ^{13}C chemical shifts were determined using residual signals of the deuterated solvents and were calibrated versus SiMe_4 . $^{31}\text{P}\{^1\text{H}\}$ NMR spectra were referenced externally to an aqueous solution of H_3PO_4 .

3.2. General Procedure for Monitoring of Hydroformylation Reactions

In a typical experiment, the desired amount of $\text{Rh}(\text{acac})(\text{CO})_2$ (as a $1.0 \text{ g}\cdot\text{L}^{-1}$ toluene solution (pale yellow)) ($1.33 \mu\text{mol}$) was added on biphephos (20.9 mg, $26.6 \mu\text{mol}$ (weighed in the glove box)) in a Schlenk flask. 10-Undecenitrile (0.661 g, 10.0 mmol) in the desired solvent (8 mL at $[\mathbf{1}]_0/[\text{Rh}] = 3000$) (toluene, acetonitrile or 1,4-dioxane) was added onto the resulting mixture (amount indicated above correspond to experiments at $[\mathbf{1}]_0/[\text{Rh}] = 3000$; for experiments at different $[\mathbf{1}]_0/[\text{Rh}]$ ratios, the amounts were adjusted). The solution was stirred at room temperature for 15 min and then transferred under argon into a 90 mL stainless-steel autoclave, equipped with a magnetic stir bar. The reactor was sealed, charged with CO/H_2 at the desired pressure at room temperature, and then heated with silicon oil set at the desired temperature ($120 \text{ }^\circ\text{C}$). During the reaction course, aliquots were sampled (ca. 1 mL of reaction mixture was purged) at regular time intervals to monitor the conversion and selectivities by ^1H NMR. After the appropriate reaction time, the reactor was cooled to room temperature and vented to atmospheric pressure. The solution was analyzed by NMR (after evaporation of solvent). The same procedure was applied for experiments with methyl-10 undecenoate and 5-hexenenitrile. For reaction with isolated $\text{RhH}(\text{biphephos})(\text{CO})_2$, the same procedure was used replacing the metallic precursor $\text{Rh}(\text{acac})(\text{CO})_2$ by the isolated species with the desired amount of biphephos.

10-Undecenenitrile (1): ^1H NMR (CDCl_3 , 400 MHz, 298 K): $\delta = 5.80$ (m, 1H, $\text{CH}=\text{CH}_2$), 4.94 (m, 2H, $\text{CH}=\text{CH}_2$), 2.33 (t, $J = 7.1$ Hz, 2H, CH_2CN), 2.09–2.03 (td, 2H, $J = 6.9$ and 1.2 Hz, $\text{CH}_2\text{CH}=\text{CH}$), 1.77–1.61 (m, 2H, $\text{CH}_2\text{CH}_2\text{CN}$), 1.55–1.23 (m, 10H, CH_2 chain) ppm.

Internal Isomers of Undecenenitrile (1-int-x): Typical signals for these internal isomers were observed in ^1H NMR (CDCl_3 , 400 MHz, 298 K) at $\delta = 5.40$ – 5.20 (m, 2H); the CH_3CH_2 signal for *cis/trans* 8-undecenenitrile was observed at $\delta = 0.92$ (t, $J = 7.3$ Hz, 3H) ppm; other ^1H signals overlap with those of 1. Same signal were observed in the case of internal isomers obtained from methyl 10-undecenoate. Alkene signals were also evidenced in $^{13}\text{C}\{^1\text{H}\}$ NMR (CDCl_3 , 100 MHz, 298K): *trans*-9-undecene $\delta = 131.3$ and 124.7 ppm; *cis*-9-undecene $\delta = 130.5$ and 123.8 ppm; *trans*-8-undecene $\delta = 132.2$ and 128.8 ppm; *cis*-8-undecene $\delta = 131.8$ and 128.8 ppm [24].

Hydroformylation Products (2) and (3) Derived from 10-Undecenenitrile: Typical signals for these aldehydes were observed in ^1H NMR (CDCl_3 , 400 MHz, 298 K) at $\delta = 9.66$ (t, $J = 2$ Hz, 1H) ppm for the linear aldehyde 2. The branched aldehyde (3) is observed at $\delta = 9.50$ (d, $J = 2$ Hz, 1H) ppm. The same signals were observed in the case of aldehydes obtained from methyl 10-undecenoate. The aldehyde signals were also evidenced in $^{13}\text{C}\{^1\text{H}\}$ NMR (CDCl_3 , 100 MHz, 298K): linear aldehyde (2): $\delta = 201.9$ ppm; branched aldehyde (3): $\delta = 204.3$ ppm.

Hydrogenation Products (4) Derived from 10-Undecenenitrile and Methyl 10-Undecenoate: Typical signal for these products were observed in ^1H NMR (CDCl_3 , 400 MHz, 298 K) at $\delta = 0.87$ (t, $J = 6.6$ Hz, 3H) ppm both for 4 and the hydrogenated product obtained from methyl 10-undecenoate.

4. Conclusions

During this work, a particular attention was paid to the monitoring and understanding of the competitive isomerization vs. hydroformylation of 10-undecenenitrile with the well-performing Rh-biphephos system. Composition profiles of each organic species over time were established. To our knowledge, such detailed kinetic monitoring of an isomerization-hydroformylation process is here reported for the first time. Under the conditions first established to optimize the catalytic productivity and reaction selectivities [18], at low catalyst loadings, hydroformylation and isomerization appeared to be parallel, competitive reactions. Unexpectedly, when the substrate-to-catalyst ratio was decreased,

different composition profiles were diagnosed. These evidenced a two-stage regime profile with, subsequently, a first period in which fast isomerization of the terminal olefin into internal olefins and then fast conversion of internal olefins into aldehydes occur, and a second final period with slow conversion of internal olefins.

Despite unsuccessful attempts to monitor the catalytic active species themselves, these observations are, in our opinion, best rationalized by the existence of different catalytic species over time. A most “valuable” species (**X**) is present in the first period, capable of fast dynamic isomerization; however, it appears to be transient and vanishes over time. This provides a rational why the “isomerization phenomenon” is not detected at high substrate-to-Rh ratios: indeed, under such conditions that require relatively long reaction times for significant conversions of **1/1-int-x**, the first “isomerization regime” lasts for just a small fraction of the overall process and impacts only a minor amount of the converted substrate; hence, no building up of internal isomers is detected.

On the other hand, the lower the undecenitrile-to-Rh ratio, the more evident and pronounced the isomerization phenomenon is. Our experiments revealed another important aspect: the isomerization rate was much more important than the hydroformylation rate at low [biphephos]/[Rh] ratio. This may suggest that the transient initial species **X** responsible for fast isomerization may be one having no biphephos coordinated onto Rh. Additionally, internal isomers were consumed (i.e., converted into **2**) more rapidly at higher syngas pressure, making the “isomerization peak” more apparent under such conditions (Figure 6). We hypothesized that this may simply result from lower hydroformylation rates (and hence capacity to drive the equilibrium $\mathbf{1-int-x} \rightleftharpoons \mathbf{1} \rightarrow \mathbf{2}$) at relatively low CO/H₂ pressure; in turn, this would suggest no direct influence of CO/H₂ on species **X**, at least in the pressure range investigated (4–40 bar). Note that such species **X** would not be (significantly) active for hydroformylation since the regioselectivity for aldehydes is strictly identical within the two stages/regimes of the reaction, and can be, hence, ascribed unambiguously to a Rh-biphephos species (which resting state is RhH(biphephos)(CO)₂). Upon time, even more easily at high [biphephos]/[Rh] ratios, **X** would collapse to the “regular” Rh-biphephos species.

Additionally, the isomerization phenomenon proved very substrate dependent; no such effect was observed with methyl 10-undecenoate and 5-hexenenitrile. The reason for this substrate dependence remains obscure at this time. Requisite for putative bidendate coordination of undecenitrile to generate the active species **X** seems unlikely as it may also be anticipated to proceed with hexenenitrile.

Acknowledgments: This work was supported by the French National Research Agency, ANR project MEMCHEM (14-CE06-0022-02) and Arkema Co. We are indebted to Carmen Claver and Cyril Godard from the University of Tarragona for extensive high pressure ³¹P NMR investigations of those reactions. We are most grateful to David Sémeril and Dominique Matt from the University of Strasbourg for a generous gift of the calixarene-bisphosphite ligand L2. We gratefully thank Umicore Co. (Angelino Doppiu) for a generous gift of Rh(acac)(CO)₂.

Author Contributions: Lucas Le Goanvic and Jean-François Carpentier conceived and designed the experiments; Lucas Le Goanvic performed the experiments; Lucas Le Goanvic and Jean-François Carpentier analyzed the data; Jean-Luc Couturier and Jean-Luc Dubois contributed to the discussions, reagents/materials and analysis; and Lucas Le Goanvic and Jean-François Carpentier wrote the paper.

Conflicts of Interest: The authors declare no conflict of interest.

Appendix A

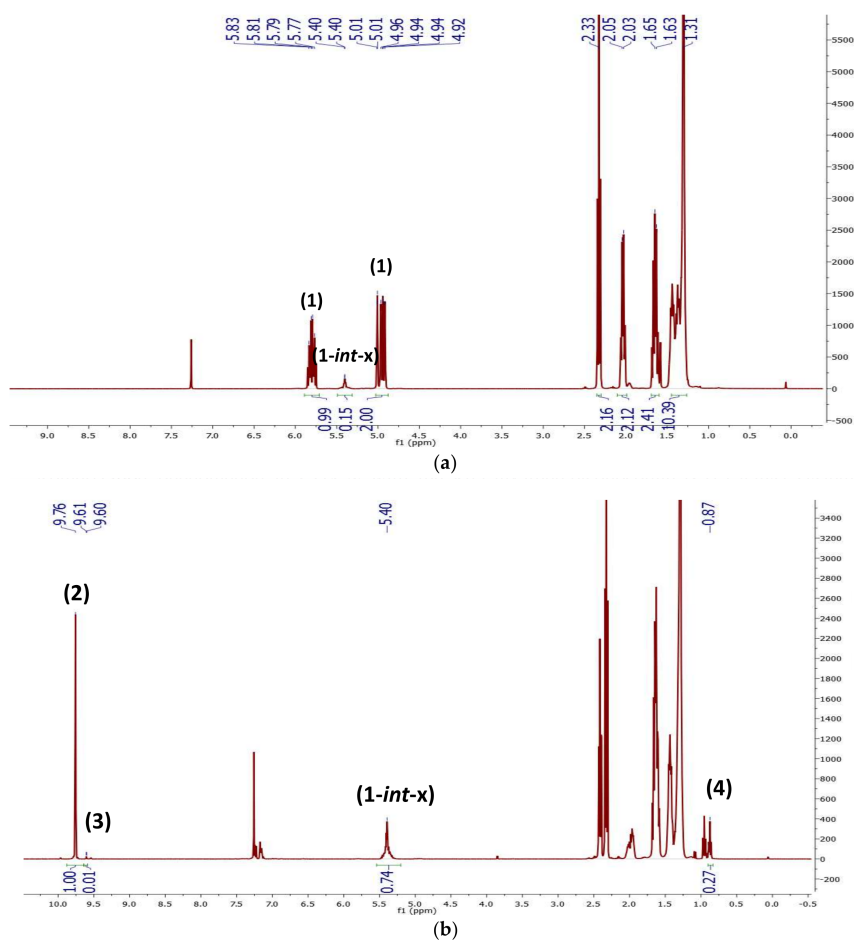


Figure A1. ^1H NMR spectrum (400 MHz, CDCl_3 , 23 °C): (a) starting material 1/1-int-x; and (b) reaction mixture at 100% conversion of 1 (bottom) (Table 1, entry 1).

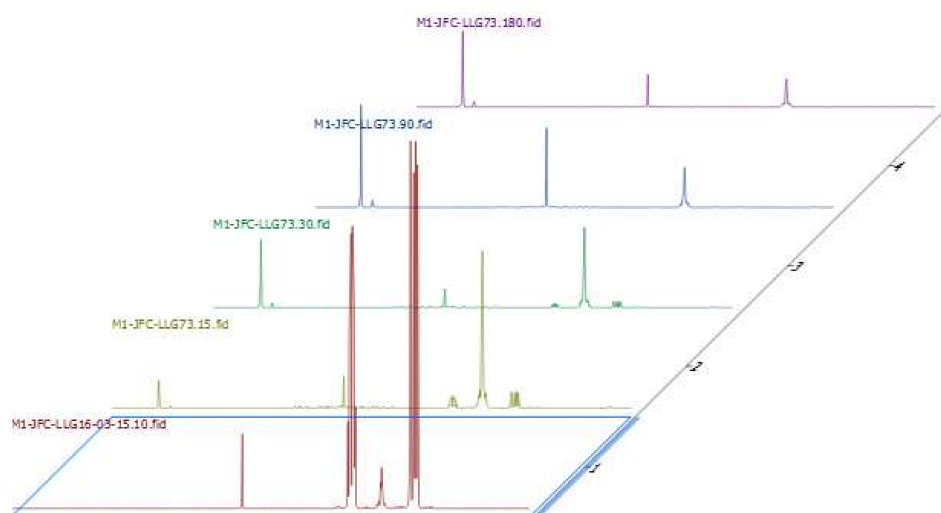


Figure A2. ^1H NMR (400 MHz, CDCl_3 , 298 K) monitoring of a reaction mixture over time during an isomerization phenomenon in CH_3CN with the Rh-calixarene-bisphosphite (**L2**) catalyst system (conditions: $1/1\text{-int-x}$ (93.5:6.5) = 3.15 mmol, $[1]_0 = 0.4$ M, $[1]_0/[Rh] = 3000$, $[L2]_0/[Rh] = 20$, $P = 20$ bar ($\text{CO}/\text{H}_2 = 1:1$), MeCN (8 mL), $T = 120$ °C).

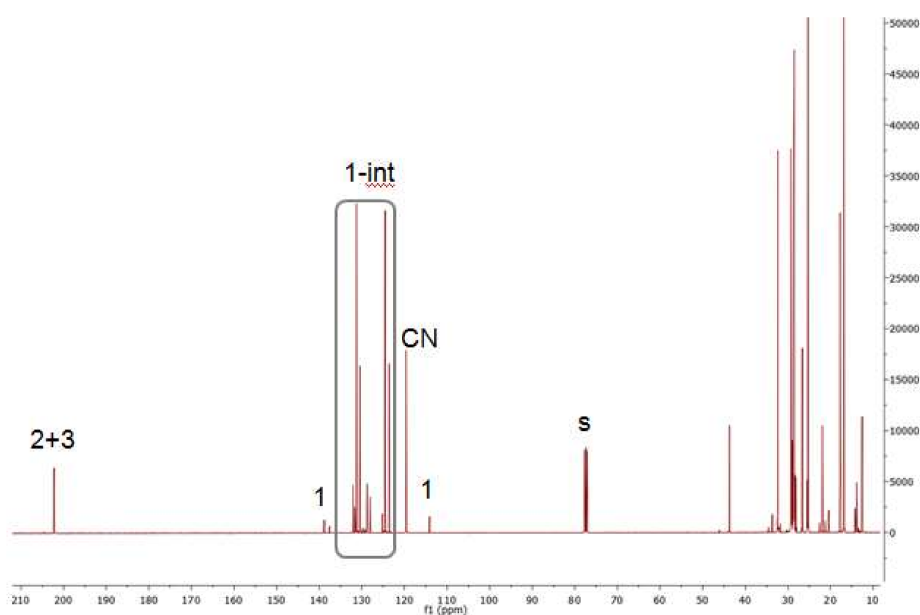


Figure A3. $^{13}\text{C}\{^1\text{H}\}$ NMR spectrum (100 MHz, CDCl_3 , 298 K) of a reaction mixture evidencing an “isomerization peak” (Table 2, entry 8). The important amount of internal olefins **1-int-x** is easily observed.

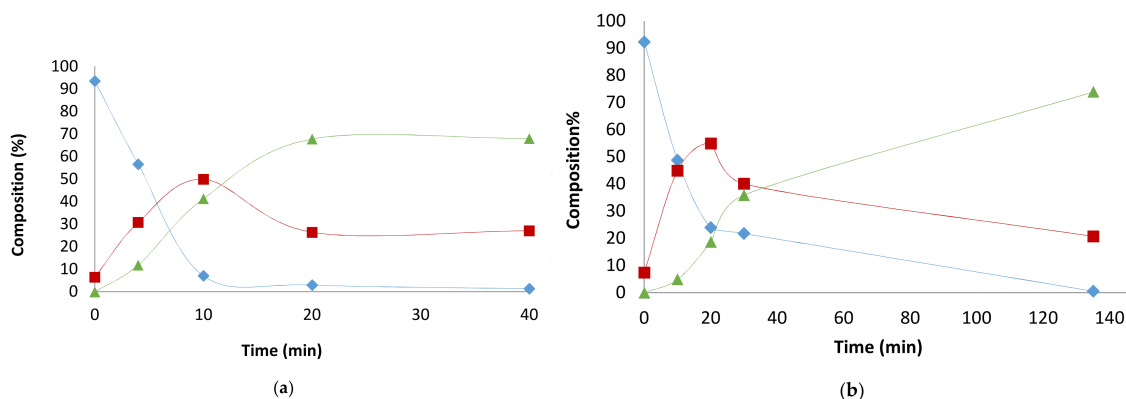


Figure A4. Composition profiles as a function of time at $[1]_0/[Rh] = 3000$: (a) acetonitrile; and (b) 1,4-dioxane (\blacklozenge 1, \blacksquare 1-int-x, \blacktriangle 2 + 3) (Table 2, entries 8 and 9).

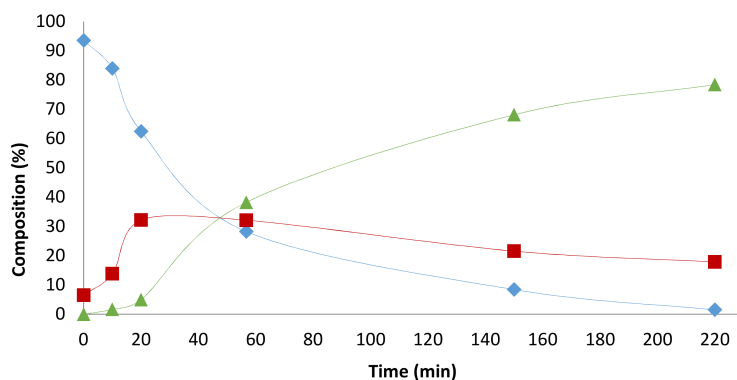


Figure A5. Composition profiles during the tandem hydroformylation-isomerization of 10-undecenitrile with Rh-biphephos in toluene at $[1]_0/[Rh] = 3000$ at 30 bar CO + 10 bar H₂ (\blacklozenge 1, \blacksquare 1-int-x, \blacktriangle 2 + 3) (Table 3, entry 14).

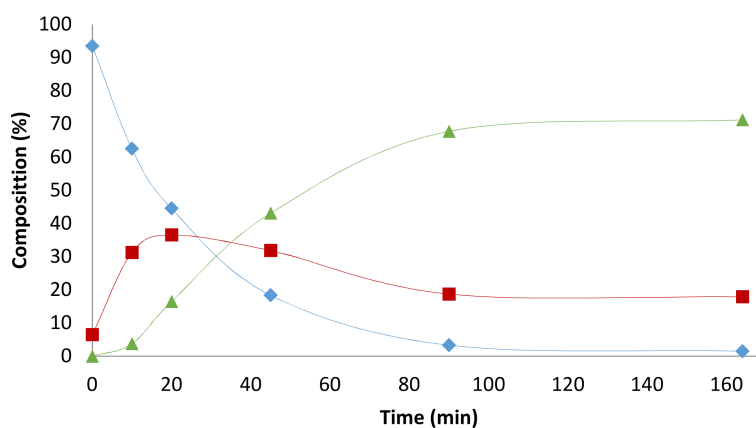


Figure A6. Composition profiles during the tandem hydroformylation-isomerization of 10-undecenitrile with Rh-biphephos in toluene at $[1]_0/[Rh] = 3000$ at 10 bar CO + 30 bar H₂ (\blacklozenge 1, \blacksquare 1-int-x, \blacktriangle 2 + 3) (Table 3, entry 15).

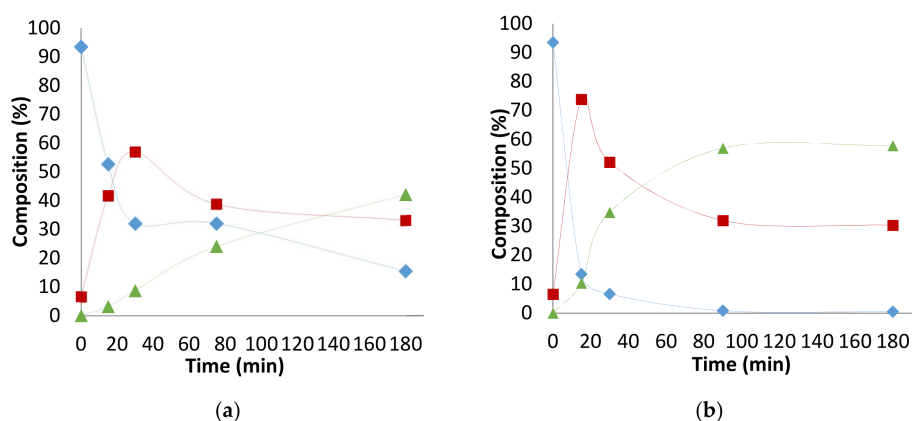


Figure A7. Composition profiles as a function of time with Rh-L2 system at $[1]_0/[Rh] = 3000$: (a) toluene; (b) acetonitrile (\diamond 1, \blacksquare 1-int-x, \blacktriangle 2 + 3) (conditions: 1/1-int-x (93.5:6.5) = 3.15 mmol, $[1]_0 = 0.4$ M, $[1]_0/[Rh] = 3000$, $[L2]_0/[Rh] = 20$, $P = 20$ bar (CO/H₂ = 1:1), solvent (8 mL), $T = 120$ °C).

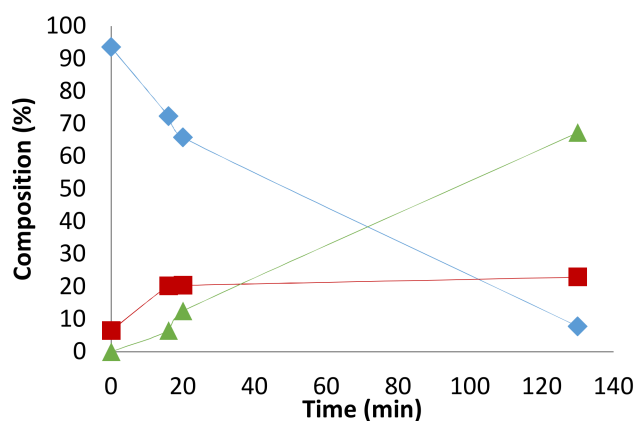


Figure A8. Composition profiles as a function of time with Rh-A4N3 system at $[1]_0/[Rh] = 3000$ in toluene (\diamond 1, \blacksquare 1-int-x, \blacktriangle 2 + 3) (conditions: 1/1-int-x (93.5:6.5) = 3.15 mmol, $[1]_0 = 0.4$ M, $[1]_0/[Rh] = 3000$, $[ligand]_0/[Rh] = 20$, $P = 20$ bar (CO/H₂ = 1:1), solvent (8 mL), $T = 120$ °C).

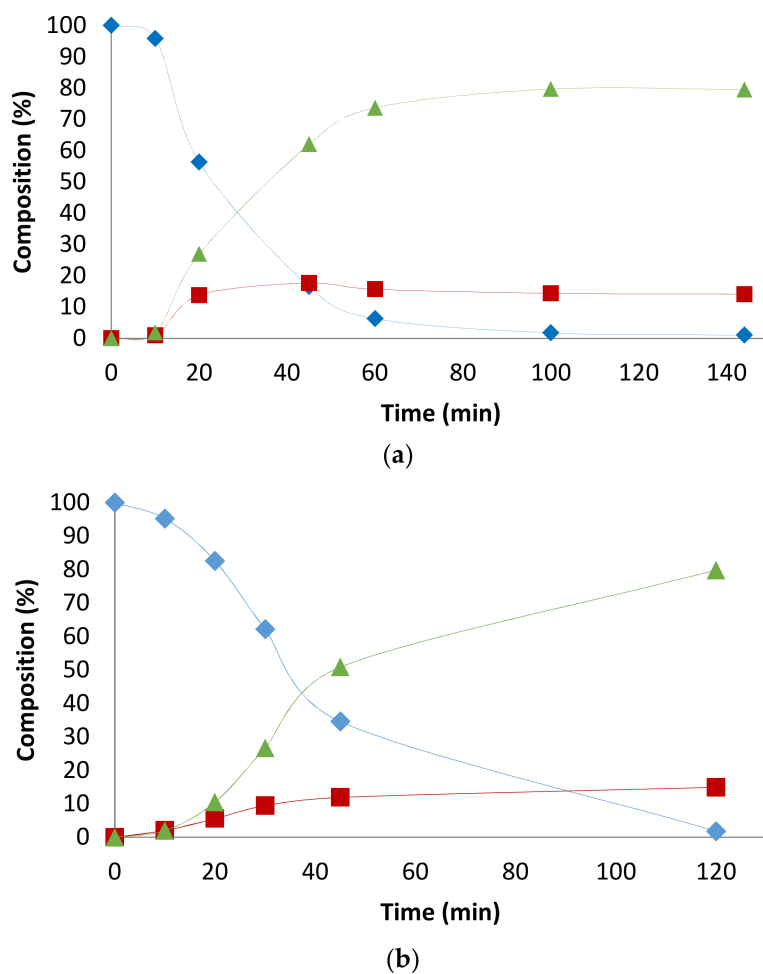


Figure A9. Composition profiles at $[\text{substrate}]_0/[\text{Rh}] = 3000$ with methyl 10-undecenoate: (a) toluene; (b) acetonitrile (\blacklozenge 1^{Me} , \blacksquare $1^{\text{Me-int-x}}$, \blacktriangle $2^{\text{Me}} + 3^{\text{Me}}$) (conditions : $1^{\text{Me}} = 3.15$ mmol, $[1^{\text{Me}}]_0 = 0.4$ M, $[1^{\text{Me}}]_0/[\text{Rh}] = 3000$, $[\text{biphephos}]_0/[\text{Rh}] = 20$, $P = 20$ bar ($\text{CO}/\text{H}_2 = 1:1$), solvent (8 mL), $T = 120$ °C).

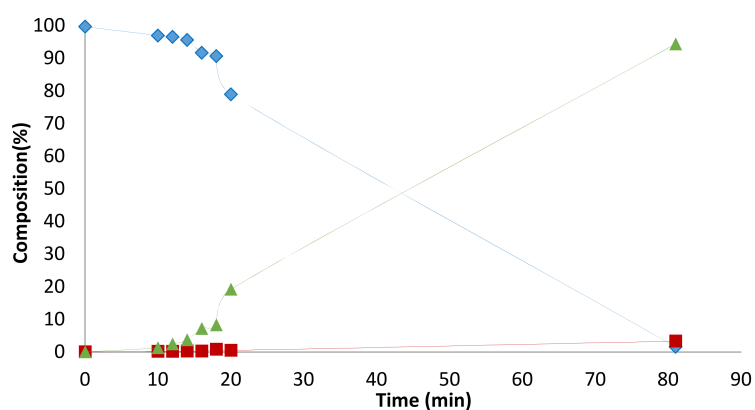


Figure A10. Composition profile at $[\text{substrate}]_0/[\text{Rh}] = 3000$ with 5-hexenenitrile in toluene (\blacklozenge 1^{Hex} , \blacksquare $1^{\text{Hex-int-x}}$, \blacktriangle $2^{\text{Hex}} + 3^{\text{Hex}}$). (conditions: $1^{\text{Hex}} = 3.15$ mmol, $[1^{\text{Hex}}]_0 = 0.4$ M, $[1^{\text{Hex}}]_0/[\text{Rh}] = 3000$, $[\text{biphephos}]_0/[\text{Rh}] = 20$, $P = 20$ bar ($\text{CO}/\text{H}_2 = 1:1$), solvent (8 mL), $T = 120$ °C).

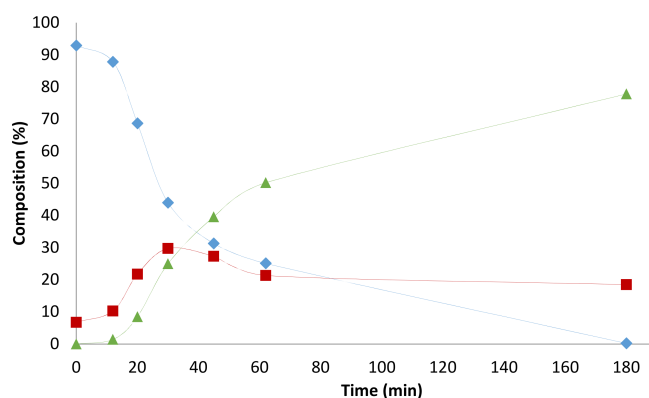


Figure A11. Composition profiles as a function of time at $[1]_0/[Rh] = 3000$ with 10-undecenitrile heated at $150\text{ }^\circ\text{C}$ under argon prior to catalysis (\blacklozenge **1**, \blacksquare **1-int-x**, \blacktriangle **2 + 3**) (conditions : **1/1-int-x** (93.5:6.5) = 3.15 mmol, $[1]_0 = 0.4\text{ M}$, $[1]_0/[Rh] = 3000$, $[\text{biphephos}]_0/[Rh] = 20$, $P = 20\text{ bar}$ ($\text{CO}/\text{H}_2 = 1:1$), toluene (8 mL), $T = 120\text{ }^\circ\text{C}$).

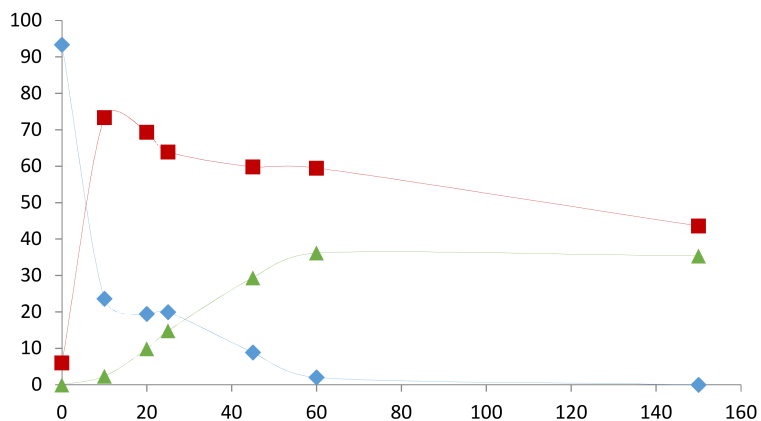


Figure A12. Composition profiles as a function of time with $\text{RhH}(\text{biphephos})(\text{CO})_2$ isolated species without ligand addition in toluene at $[1]_0/[Rh] = 3000$ (\blacklozenge **1**, \blacksquare **1-int-x**, \blacktriangle **2 + 3**) (conditions : **1/1-int-x** (93.5:6.5) = 3.15 mmol, $[1]_0 = 0.4\text{ M}$, $[1]_0/[Rh] = 3000$, $P = 20\text{ bar}$ ($\text{CO}/\text{H}_2 = 1:1$), toluene (8 mL), $T = 120\text{ }^\circ\text{C}$).

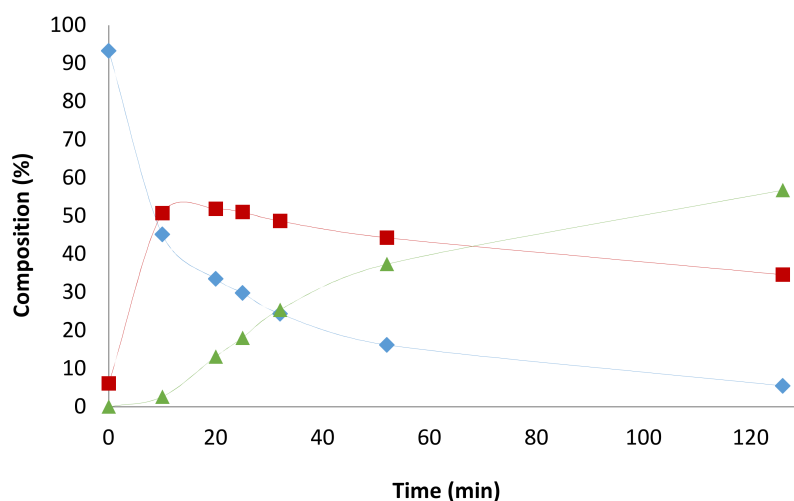


Figure A13. Composition profiles as a function of time with $\text{RhH}(\text{biphephos})(\text{CO})_2$ isolated species with ligand addition (20 equiv. vs. Rh) in toluene at $[\mathbf{1}]_0/[\text{Rh}] = 3000$ (\blacklozenge **1**, \blacksquare **1-int-x**, \blacktriangle **2 + 3**) (conditions: $\mathbf{1}/\mathbf{1-int-x}$ (93.5:6.5) = 3.15 mmol, $[\mathbf{1}]_0 = 0.4$ M, $[\mathbf{1}]_0/[\text{Rh}] = 3000$, $P = 20$ bar ($\text{CO}/\text{H}_2 = 1:1$), toluene (8 mL), $T = 120$ °C).

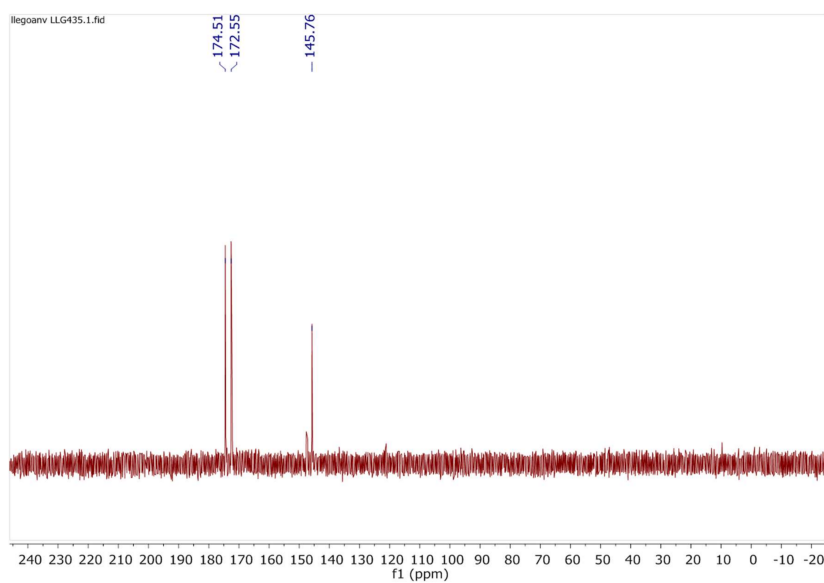


Figure A14. ^{31}P NMR (tol-d_8 , 162 MHz, 298 K) spectrum of $\text{RhH}(\text{biphephos})(\text{CO})_2$ species. The doublet at $\delta = 173.5$ ppm stands for $\text{RhH}(\text{biphephos})(\text{CO})_2$ and the signal at $\delta = 146.7$ ppm corresponds to free biphephos.

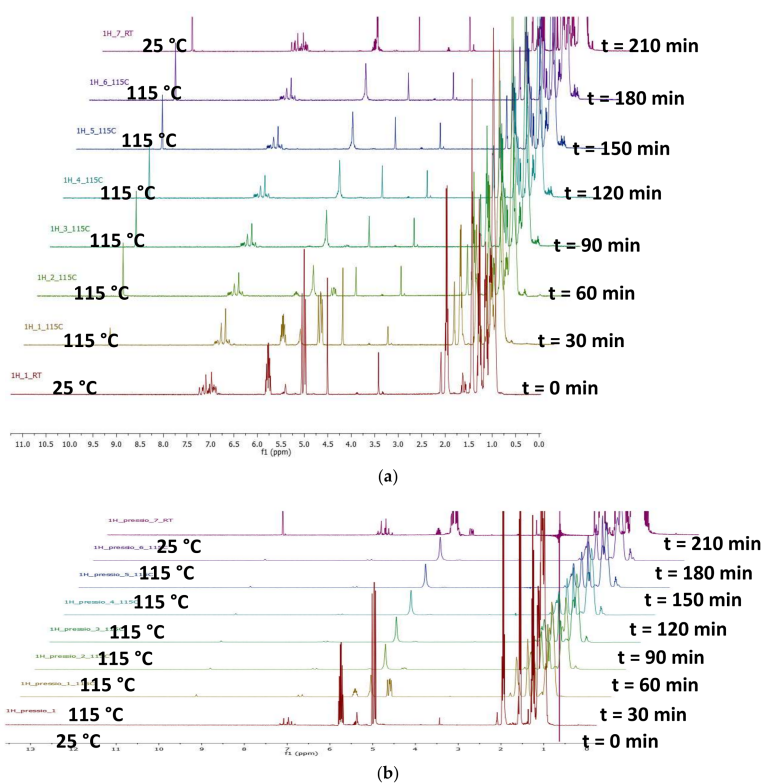


Figure A15. ^1H NMR monitoring: (a) $[\mathbf{1}]_0/[\text{Rh}] = 20,000$, $[\mathbf{1}]_0 = 1.0 \text{ M}$; and (b) $[\mathbf{1}]_0/[\text{Rh}] = 3000$, $[\mathbf{1}]_0 = 0.4 \text{ M}$ (conditions: $[\text{biphephos}]_0/[\text{Rh}] = 20$, $P = 20 \text{ bar}$ ($\text{CO}/\text{H}_2 = 1:1$), toluene- d_8 , $T = 115 \text{ }^\circ\text{C}$).

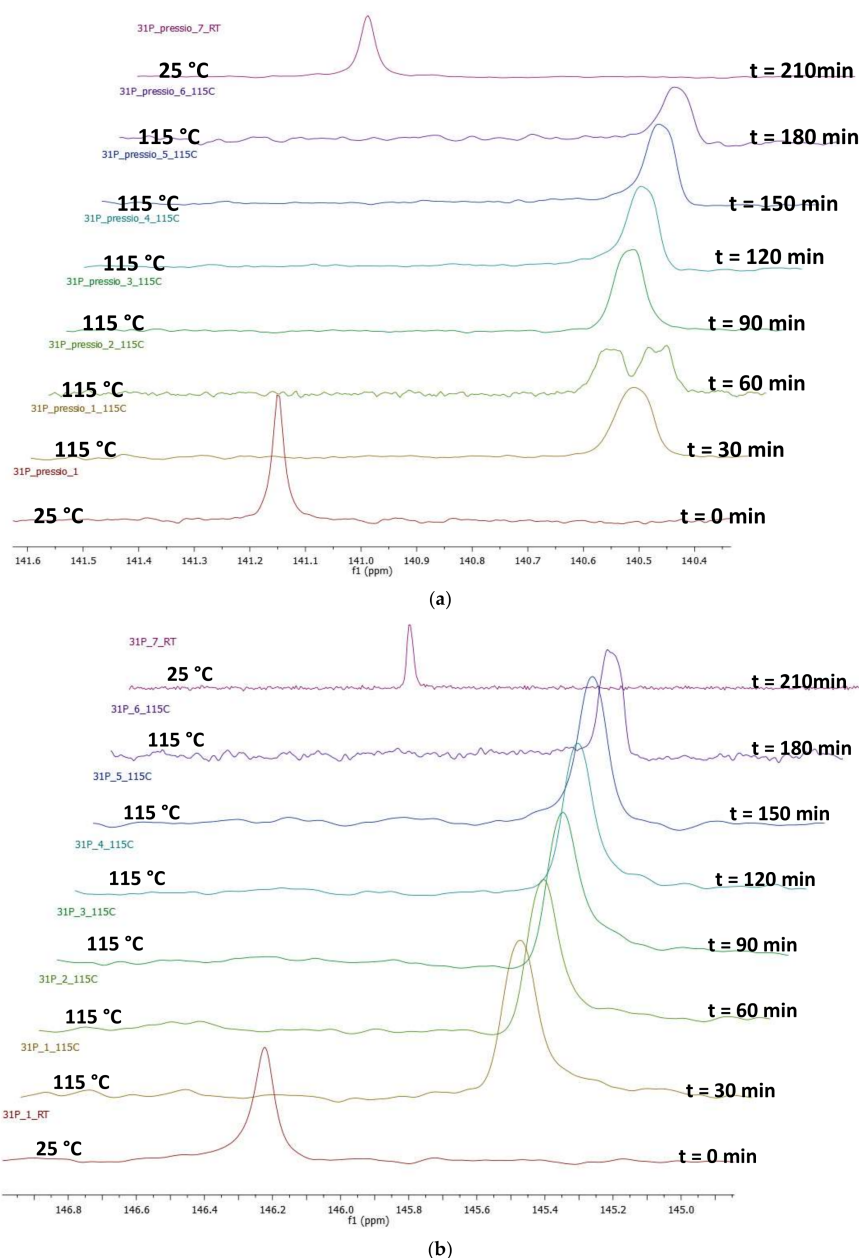


Figure A16. $^{31}\text{P}\{^1\text{H}\}$ NMR monitoring with $[\text{biphephos}]_0/[\text{Rh}] = 20$: (a) at $[\mathbf{1}]_0/[\text{Rh}] = 20,000$; and (b) at $[\mathbf{1}]_0/[\text{Rh}] = 3000$.

References

1. Kohls, E.; Stein, M. The thermochemistry of long chain olefin isomers during hydroformylation. *New J. Chem.* **2017**, *41*, 7347–7355. [[CrossRef](#)]
2. Vilches-Herrera, M.; Domke, L.; Börner, A. Isomerization-Hydroformylation tandem reactions. *ACS Catal.* **2014**, *4*, 1706–1724. [[CrossRef](#)]
3. Goldbach, V.; Roesle, P.; Mecking, S. Catalytic isomerizing ω -functionalization of fatty acids. *ACS Catal.* **2015**, *5*, 5951–5972. [[CrossRef](#)]
4. Billig, E.; Abatjoglou, A.G.; Bryant, D.R.; Union Carbide Corporation. Transition Metal Complex Catalyzed Processes. U.S. Patent 4668651, 5 September 1985.
5. Billig, E.; Abatjoglou, A.G.; Bryant, D.R.; Union Carbide Corporation. Transition Metal Complex Catalyzed Processes. European Patent 214622, 4 September 1986.

6. Billig, E.; Abatjoglou, A.G.; Bryant, D.R.; Union Carbide Corporation. Transition Metal Complex Catalyzed Processes. U.S. Patent 4769498, 6 September 1988.
7. Yan, Y.; Zhang, X.; Zhang, X. A tetraphosphorus ligand for highly regioselective isomerization-hydroformylation of internal olefins. *J. Am. Chem. Soc.* **2006**, *128*, 16058–16061. [[CrossRef](#)] [[PubMed](#)]
8. Yu, S.; Chie, Y.; Guan, Z.; Zhang, X. Highly regioselective isomerization-hydroformylation of internal olefins to linear aldehyde using Rh complexes with tetraphosphorus ligands. *Org. Lett.* **2008**, *10*, 3469–3472. [[CrossRef](#)] [[PubMed](#)]
9. Sémeril, D.; Matt, D.; Toupet, L. Highly regioselective hydroformylation with hemispherical chelators. *Chem. Eur. J.* **2008**, *14*, 7144–7155. [[CrossRef](#)] [[PubMed](#)]
10. Behr, A.; Obst, D.; Schulte, C.; Schosser, T. Highly selective tandem isomerization-hydroformylation reaction of trans-4-octene to n-nonanal with rhodium-Biphephos catalysis. *J. Mol. Catal. A Chem.* **2003**, *206*, 179–184. [[CrossRef](#)]
11. Behr, A.; Obst, D.; Schulte, C. Kinetik der isomerisierenden Hydroformylierung von trans-4-Octen. *Chem. Ing. Tech.* **2004**, *76*, 904–910. [[CrossRef](#)]
12. Behr, A.; Obst, D.; Westfechtel, A. Isomerizing hydroformylation of fatty acid esters: Formation of ω -aldehydes. *Eur. J. Lipid Sci. Technol.* **2005**, *107*, 213–219. [[CrossRef](#)]
13. Furst, M.R.L.; Korkmaz, V.; Gaide, T.; Seidensticker, T.; Behr, A.; Vorholt, A.J. Tandem reductive hydroformylation of castor oil derived substrates and catalyst recycling by selective product crystallisation. *ChemCatChem* **2017**, *9*, 4319–4323. [[CrossRef](#)]
14. Gaide, T.; Bianga, J.; Schlipköter, K.; Behr, A.; Vorholt, A.J. Linear selective isomerization/hydroformylation of unsaturated fatty acid methyl esters: A bimetallic approach. *ACS Catal.* **2017**, *7*, 4163–4171. [[CrossRef](#)]
15. Pandey, S.; Chikkali, S.H. Highly regioselective isomerizing hydroformylation of long-chain internal olefins catalyzed by a rhodium bis(phosphite) complex. *ChemCatChem* **2015**, *7*, 3468–3471. [[CrossRef](#)]
16. Pandey, S.; Shinde, D.R.; Chikkali, S.H. Isomerizing hydroformylation of cashew nut shell liquid. *ChemCatChem* **2017**, *9*, 3997–4004. [[CrossRef](#)]
17. Yuki, Y.; Takahashi, K.; Tanaka, Y.; Nozaki, K. Tandem isomerization-hydroformylation-hydrogenation of internal alkenes to n-alcohols using Rh/Ru dual- or ternary-catalyst systems. *J. Am. Chem. Soc.* **2013**, *135*, 17393–17400. [[CrossRef](#)] [[PubMed](#)]
18. Ternel, J.; Couturier, J.-L.; Dubois, J.-L.; Carpentier, J.-F. Rhodium-catalyzed tandem isomerization-hydroformylation of the bio-sourced 10-Undecenitrile: Selective and productive catalysts for production of polyamide-12 precursor. *Adv. Synth. Catal.* **2013**, *355*, 3191–3204. [[CrossRef](#)]
19. Le Goanvic, L.; Couturier, J.-L.; Dubois, J.-L.; Carpentier, J.-F. Ruthenium-catalyzed hydroformylation of the functional unsaturated fatty nitrile 10-undecenitrile. *J. Mol. Catal. A Chem.* **2016**, *417*, 116–121. [[CrossRef](#)]
20. Dubois, J.-L.; Gillet, J.-P. Coproduction of Cyclic Carbonates and of Nitriles and/or Fatty Amines. WO Patent 2008/145941A2, 4 December 2008.
21. Ternel, J.; Couturier, J.-L.; Dubois, J.-L.; Carpentier, J.-F. Rhodium versus iridium catalysts in the controlled tandem hydroformylation–isomerization of functionalized unsaturated fatty substrates. *ChemCatChem* **2015**, *7*, 513–520. [[CrossRef](#)]
22. Claver, C.; van Leeuwen, P.W.N.M. *Rhodium Catalyzed Hydroformylation*; Springer: Berlin, Germany, 2008.
23. Monnerneau, L.; Sémeril, D.; Matt, D. Solvent-free olefin hydroformylation using hemispherical diphosphites. *Eur. J. Org. Chem.* **2010**, *16*, 3068–3073. [[CrossRef](#)]
24. Gunstone, F.D.; Pollard, M.R.; Scrimgeour, C.M.; Vedanayagam, H.S. ¹³C nuclear magnetic resonance studies of olefinic fatty acids and esters. *Chem. Phys. Lipids* **1977**, *18*, 115–129. [[CrossRef](#)]

